Chemical Engineering Journal 165 (2010) 686–692

Contents lists available at ScienceDirect

Chemical Engineering Journal

journal homepage: www.elsevier.com/locate/cej

Direct synthesis of dimethyl carbonate over activated carbon supported Cu-based catalysts

J. Bian [a,*], X.W. Wei [a], Y.R. Jin [a], L. Wang [a], D.C. Luan [a], Z.P. Guan [b]

[a] Key Laboratory of Special Materials and Preparation Technologies, School of Materials Science & Engineering, Xi-hua University, 999 Jinzhou Road, Chengdu, Sichuan 610039, People's Republic of China
[b] Department of Chemistry, National University of Singapore, 3 Science Drive 3, Singapore 117543, Republic of Singapore

ARTICLE INFO

Article history:
Received 2 April 2010
Received in revised form
24 September 2010
Accepted 2 October 2010

Keywords:
Dimethyl carbonate
Methanol
Carbon dioxide
Cu-based catalysts
Catalysis

ABSTRACT

A series of Cu-based catalysts have been synthesized by the conventional incipient wetness impregnation and utilized in the dimethyl carbonate (DMC) synthesis. The effects of preparation and reaction conditions on the catalytic activities were intensively investigated. The surface properties and morphology of the employed catalysts were fully characterized using TPD-NH_3, XRD, SEM-EDX, TEM and XPS techniques. Structural investigation indicated that Cu^0, Cu^+ and Cu^{2+} co-existed on the surface of employed catalyst and they were the main active species in DMC synthesis. Calcining the catalyst at proper temperature could promote the formation of active species, hence the activity of $CuCl_2$/AC catalyst. Maintaining proper and effective Cu structure on AC surface will promote more selective DMC formation. Catalytic evaluation suggested that regardless of catalyst compositions, the optimal reaction conditions for DMC synthesis were found to be 393 K and 1.2 MPa. DMC formation rate was strongly related to the Cu loading, calcination temperature and Cl/Cu ratio. Under the optimal conditions of 7 wt% Cu loading and 673 K calcination, the highest DMC formation rate of 4.77 mmol h^{-1} and DMC selectivity of 90.1% could be achieved, respectively.

1. Introduction

Dimethyl carbonate (DMC), an environmentally building block, can be used as fuel additives, carbonylating agents, alkylating agents and polar solvents [1]. Moreover, DMC exhibits wide applications in the synthesis of polycarbonate and polyurethane [1]. Several commercial processes have been developed for the synthesis of DMC, including the methanolysis of phosgene [2], oxidative carbonylation of methanol [3] and transesterification route [4]. However, these processes have some shortcomings. In contrast, direct synthesis of DMC from CH_3OH and CO_2 is a much more attractive method since such an approach is environmentally benign by nature.

A number of catalysts have been reported to be effective in this reaction, such as organometallic compounds [5], metal tetraalkoxides [6], potassium carbonate [7], ZrO_2 [8], $H_3PW_{12}O_4$–ZrO_2 [9], H_3PO_4–V_2O_5 [10], Cu–Ni/VSO [11] and Cu–(Ni,V,O)/SiO_2 [12]. However, the formation rate of DMC was reported to be low, even in the presence of dehydrates and additives such as $CaCl_2$ [13], 2,2-dimethoxy propane (DMP) [14], molecular sieves [15] and UV-light assistance [12]. Also, this reaction has been performed under supercritical conditions [16]. But, the rigorous method is difficult to control. Therefore, exploitation of novel catalysts which have highly catalytic activity is still main issue to be tackled.

The supported transition metal particles exhibit high catalytic effects in DMC synthesis [11,12]. To develop efficient catalytic systems, more efforts have been devoted to the uses of various metals as catalysts. However, the support employed in the catalytic system is much less explored. To date, the supports of loaded catalysts used in direct synthesis of DMC are mainly inorganic oxides or compound oxides, including SiO_2 [12,17], ZrO_2 [8,9], MgO–SiO_2 (MgSiO) [18], V_2O_5–SiO_2 (VSO) [11] and ZrO_2–CeO_2 [14]. While these conventional materials offer some remarkable features as catalyst supports, they suffer from major shortcomings in that they have a relatively low surface area, high cost, low activity and short longevity of final catalysts. Therefore, development of novel supports with the required properties from inexpensive raw materials is highly desired.

Carbonaceous materials have been widely applied in catalysis (either as supports or as catalysts on their own) because of their superior structural, mechanical, chemical, thermal, and unique electrical transporting properties [19]. Especially, AC is being touted as a versatile support for transitional metal in heterogonous catalysis. Dow chemicals reported that AC supports had greater activity, selectivity, and longevity than oxide supports

* Corresponding author. Tel.: +86 28 87726505; fax: +86 28 87720514.
E-mail addresses: bianjun2003@163.com (J. Bian), nusguanzhp@hotmail.com (Z.P. Guan).

1385-8947/$ – see front matter © 2010 Elsevier B.V. All rights reserved.
doi:10.1016/j.cej.2010.10.002

(SiO_2, TiO_2, MgO, ZnO, and Al_2O_3). It has been also reported that the oxide ions (or hydroxyls) of inorganic supports destabilized the active species more than AC supports. Furthermore, Cu-based catalysts are generally known as very active for CO_2-involved reactions, and several research results concerning CO_2 adsorption on Cu-based surfaces have been reported [20,21]. Recently, AC supported cupric chloride is one of the catalysts under intensive investigation, including CuCl/AC [22,17], $CuCl_2$–$PdCl_2$/AC [23], CuCl/composite supports, $[Cu(OCH_3)(pyridine)Cl]_2$/AC [24], and so on [25–27]. They have been used for DMC synthesis by oxidative carbonylation of methanol ($CH_3OH + O_2 + CO$). It has been found that the Cu (I) catalyst prepared by the solid-state ion-exchange method showed high DMC selectivity but low CH_3OH conversion, also $[Cu(OCH_3)(pyridine)Cl]_2$ supported on AC catalysts showed the highest activity [24]. Another catalyst which is active in $CH_3OH + O_2 + CO$ route is $CuCl_2$/AC. The catalyst showed high CH_3OH conversion with DMC selectivity of 80–90% [28], and the catalytic activity could be improved by the addition of palladium chloride or potassium acetate [23]. However, the catalyst has a serious deactivation problem.

Despite all the efforts in examining AC supported Cu catalysts for the oxidative carbonylation of methanol, little is performed on $CuCl_2$/AC catalyst in one-step synthesis of DMC. Our previous works have demonstrated that Cu–Ni bimetallic composite catalysts supported on carbonaceous materials were effective in one-step synthesis of DMC [29–32]. Herein, a series of Cu-based catalysts were synthesized and utilized in one-step direct synthesis of DMC. The preparation conditions, evaluating parameters and the surface structure are the principle experimental variable studied in this investigation. The effects of Cu loading, calcination temperature in preparing the catalysts, and the time-on-stream in activity evaluating on the surface structure and activity of catalyst are reported. It has been found that the prepared catalysts were highly efficient in one-step direct synthesis of DMC under optimal conditions.

2. Experimental

2.1. Catalyst synthesis

In order to eliminate the mineral impurities and improve the hydrophilicity, the commercial AC (supplied by Xinhua Chemical Plant, China) was first treated with 4 mol/L H_2SO_4 aqueous solution, followed by washing exhaustively with distilled water and drying in air at 373–383 K overnight. The as-received AC, with a BET surface area of 1002 m^2/g and an average pore diameter of 2.6 nm and a total pore volume of 0.58 cm^3/g, was used as catalytic support. Activated carbon supported $CuCl_2$ catalysts (denoted as $CuCl_2$/AC) were prepared by impregnating AC with $CuCl_2 \cdot 2H_2O$ aqueous solution. Water was removed by heating, and drying was carried out for 12 h at 383 K until the weight was invariable, then $CuCl_2$/AC catalyst precursor was obtained. The as-made $CuCl_2$/AC sample was then calcined at a temperature varied from 573 to 873 K for 3 h at a heating rate of 5 K/min in pure N_2 flow. The total Cu loading varied from 1.0 to 20.0 wt%.

2.2. Catalyst characterization

2.2.1. Temperature programmed desorption of ammonia ($TPD\text{-}NH_3$)

$TPD\text{-}NH_3$ experiments of catalysts were carried out in a U-shaped Pyrex tube furnace with helium as the carrier gas and pure NH_3 as adsorption gas. Typically, the sample, weighed 0.01 g, was first degassed at 523 K under helium flow (70 mL/min) for 1 h. After the degassing, the temperature of the sample was lowered to 327 K. NH_3 (80 mL/min, 99.999% purity) was then introduced to the sample cell to allow the sample to adsorb NH_3 for 1 h. After the adsorption, the gas to the sample cell was switched to helium (70 mL/min) again. At the same time, the heater was turned on and the temperature of the sample was controlled to raise from 327 to 673 K at a heating rate of 8 K/min. The NH_3 released from the sample, as a consequence of the temperature rise, was continuously monitored by a thermal conductivity detector (TCD).

2.2.2. Powder X-ray diffraction (XRD)

XRD analysis was conducted on a X'Pert Pro X-ray diffractometer (Philips). The working voltage and the current for the analyses were 40 kV and 100 mA, respectively. Cu (Kα) (0.15406 nm) was used as the light source. The sample was hold to the holder by paraffin wax and was scanned from 10° to 70° at a rate of 5°/min. The intensity data were collected covering two angles between 5° and 70° with a 0.02° step size and a counting time of 1 s per point. The crystalline phases were identified by JCPDS data bank.

2.2.3. Scanning electron microscopy (SEM)

The images of SEM were taken by using a JEOL JSM-5900LV microscope. Elemental analysis was performed by energy dispersive X-ray (EDX) instrument with the SEM apparatus.

2.2.4. Transmission electron microscopy (TEM)

The morphology, size and size distribution of active particles dispersed on the surface were examined by transmission electron microscope (Tecnai G^2 F20 S-TWIN). The accelerating voltage was 200 kV. Sample preparation for TEM examination involved the ultrasonic dispersion of the sample in ethanol and placing a drop of the suspension on a copper grid, followed by solvent evaporation. Several TEM micrographs were recorded and analyzed for particle size distribution. At least 100 active particles per sample were measured and analyzed to determine their sizes and size distributions.

2.2.5. X-ray photoelectron spectrum (XPS)

X-ray photoelectron spectrum (XPS) of sample was obtained by using a XSAM800SERIES800SINS analyzer. The used Al (Kα) radiation (1486.6 eV, 15 kV, and 150 W) was monochromatized. Survey scan spectra in the 1100–0 eV binding energy range were recorded with pass energy of 20.0 eV.

2.3. Catalyst evaluation

On-step catalytic DMC synthesis from CH_3OH and CO_2 was performed in a fixed bed flow reaction system. A micro-feeder was attached in order to supply CH_3OH. Standard reaction conditions were: $n(CH_3OH)/n(CO_2) = 2/1$, reaction temperature 373–413 K, total pressure 1.0–1.4 MPa, catalyst weight 3.0 g. CH_3OH (>99.8%) and CO_2 (99.95%) were used without further purification.

Typically, the catalyst sample was filled and sealed in the reactor. The temperature of catalyst bed in the reactor was measured by a thermocouple and controlled with a precision of ±1 K by a temperature controller. The reaction pressure was measured by digital pressure indicator and maintained constant by back pressure regulator. CH_3OH was introduced using HPLC pump to the pre-heater, where it was vaporized and then entered the reactor together with CO_2. The flow rate of reactants was controlled by mass flow controller. The reaction products were collected and introduced into an on-line GC (GC7890F) equipped with a TCD and a flame ionization detector (FID) to analyze the composition and concentration. Gaseous product (CO) was detected using TCD, while other liquid products were detected and analyzed using TCD and FID, respectively. The peaks observed in FID-GC were also identified with gas chromatograph mass spectrometer (GCMS-QP2010 plus, SHIMADZU) apparatus. Products analyzed on this sampling were DMC,

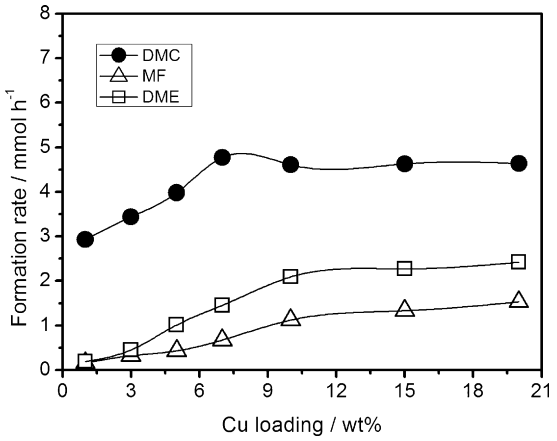

Fig. 1. Dependence of steady-state activity of DMC synthesis over $CuCl_2$/AC catalysts on Cu loading. Reaction conditions: T = 393 K; p = 1.3 MPa; CH_3OH/CO_2 = 2/1; catalyst weight 3.0 g; time-on-stream 4 h.

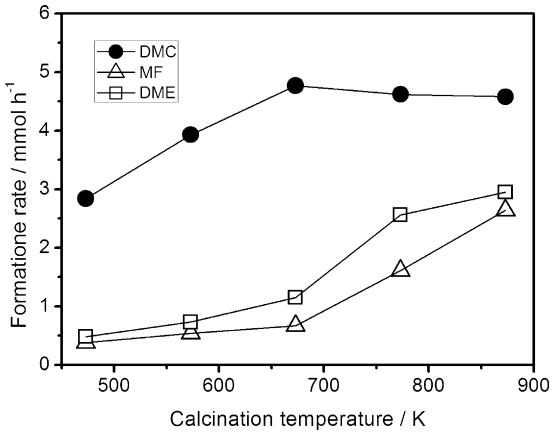

Fig. 2. Dependence of steady-state activity of DMC synthesis over $CuCl_2$/AC catalysts on calcination temperature. Reaction conditions: T = 393 K; p = 1.3 MPa; CH_3OH/CO_2 = 2/1; catalyst weight 3.0 g; time-on-stream 4 h.

methyl formate $HCOOCH_3$ (MF), a very small amount of dimethyl ether CH_3OCH_3 (DME), CO and H_2O.

3. Results and discussion

3.1. Catalyst performance in the direct synthesis of DMC from CH_3OH and CO_2

3.1.1. Effects of preparation conditions

Fig. 1 shows the dependence of steady-state activity on Cu loading of $CuCl_2$/AC catalysts. The Cu content varied from 1.0 to 20.0 wt%. In case no $CuCl_2$ was loaded on AC, the reaction did not take place at all. With the increase of Cu content, the DMC formation rate was found to increase in the entire range of evaluation. But the effect of Cu content increment on the catalytic activity was not so eminent when the Cu loadings were higher than 7 wt%. The formation rate did not increase with higher Cu loading, likely due to the decrease of active sites resulted from aggregation of metals particles and structure changes of catalysts. At the Cu content of 3, 7, 10 and 20 wt%, the DMC formation rate was found to be 3.44, 4.77, 4.61 and 4.64 mmol h^{-1}, respectively. Thus, the optimal Cu loading in catalyst for DMC synthesis reaction was thought to be 7 wt% in the economical viewpoint. The major by-products were DME, CO, MF and H_2O in this reaction. Presumably, CO was resulted from the cleavage of C–O bond of CO_2^- species [31,32], while MF was formed by the reaction of CH_3OH and HCOOH. HCOOH was formed through the oxidation of CH_3OH, as described below. These were supported by the results that DME and MF were also produced when CH_3OH and air was fed to the catalyst.

$$2CH_3OH \rightarrow (CH_3)_2O + H_2O$$

$$CH_3OH \xrightarrow{+O} HCHO \xrightarrow{+O} HCOOH \xrightarrow{+CH_3OH} HCOOCH_3$$

Fig. 2 shows the effects of calcination temperatures on the steady-state activity. It could be seen that the DMC formation rate increased with the increasing calcination temperature. When calcination temperature increased from 473 to 673 K, DMC formation rate increased from 2.75 to 4.77 mmol h^{-1}. Probably, the increasing calcination temperature was benefit to the formation of surface active species and improved their dispersion. However, the increasing trend levelled off when calcination temperature was higher than 673 K, indicating that higher calcination temperature would have no significant effect on the reaction. By further analysis we could see that DME and MF also increased continuously with the increasing calcination temperature. The increase of DME and MF would lead to the decrease of DMC selectivity. This observation illustrated that surface species on the catalyst formed during calcination had an important effect on the products formation. This result will be further proved by the following tests.

3.1.2. Effects of catalytic reaction conditions

Fig. 3 shows the dependence of steady-state catalytic activity on reaction conditions. In Fig. 3A, the reaction temperature varied from 373 to 413 K. The reaction hardly took place below 343 K

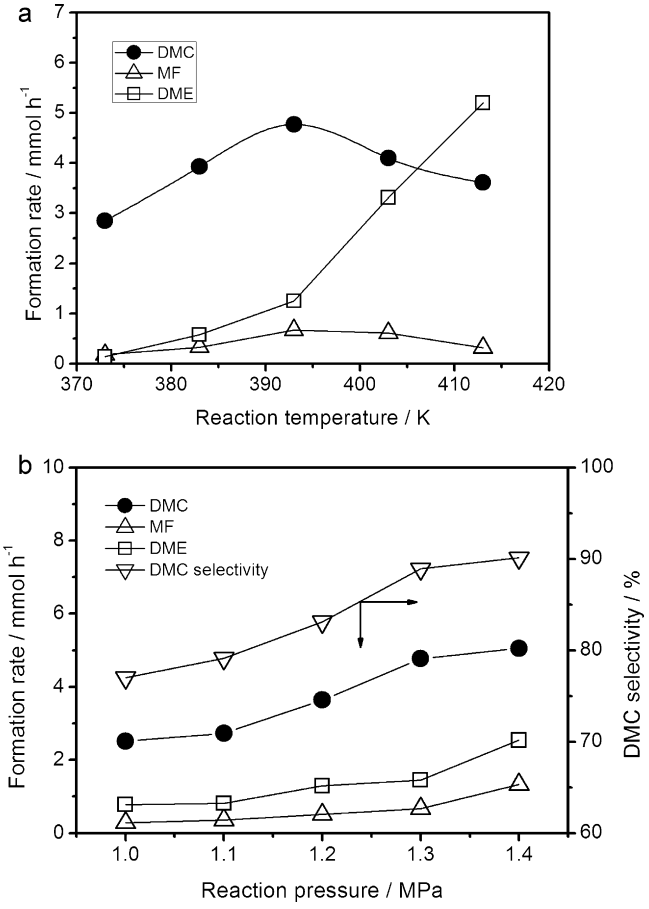

Fig. 3. Dependence of steady-state catalytic activity on reaction temperature ((A), p = 1.2 MPa) and pressure ((B), T = 393 K) over $CuCl_2$/AC catalyst (Cu: 7 wt%): CH_3OH/CO_2 = 2/1; catalyst weight 3.0 g; time-on-stream 4 h.

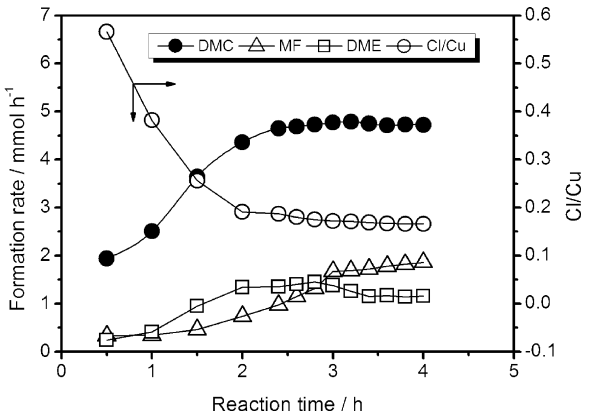

Fig. 4. Dependence of formation rate and Cl/Cu atomic ratio obtained by EDX on time-on-stream over $CuCl_2$/AC catalyst (Cu: 7 wt%). Reaction conditions: T = 393 K; p = 1.2 MPa; CH_3OH/CO_2 = 2/1; catalyst weight 3.0 g.

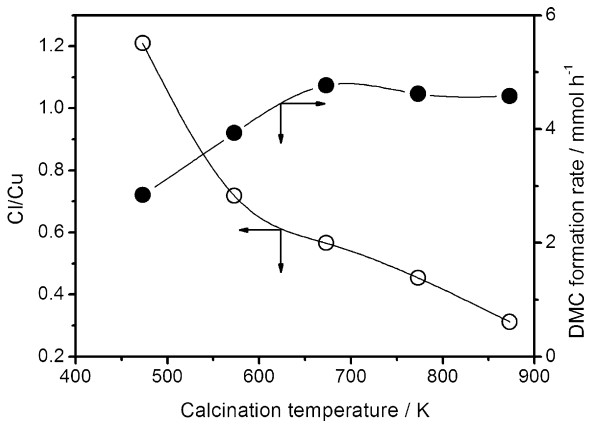

Fig. 5. Effects of calcination temperature on the Cl/Cu ratio (by EDX) and catalytic activity of $CuCl_2$/AC catalyst (Cu: 7 wt%). Reaction conditions: T = 393 K, p = 1.2 MPa, CH_3OH/CO_2 = 2/1; catalyst weight 3.0 g; time-on-stream 4 h.

and only a trace amount of reaction products were detected. On the other hand, too much by-products were produced above 423 K. Especially, as liquid by-products, DME and DMF were formed at a higher temperature by the direct reaction of CH_3OH with HCHO and HCOOH. At a lower temperature, DMC formation was enhanced with increasing temperature. But at a higher temperature than 393 K, DMC formation rate decreased gradually and DME formation rate increased drastically. Such a lower reaction temperature was suitable for higher selectivity to DMC formation. Considering the reaction rate and the selectivity of DMC, the optimal temperature condition for DMC synthesis was thought to be around 393–403 K. The effect of reaction pressure on the products formation and DMC selectivity is shown in Fig. 3B. The reaction pressure varied in the range of 1.0–1.4 MPa and the temperature was maintained at 393 K. The pressure was found to play an important role in the reaction. DMC was hardly produced at the atmospheric pressure, but its production rate increased continuously with the increase of reaction pressure. The DMC formation rate at 1.4 MPa was about two times more than that at 1.0 MPa. The selectivity of DMC was also markedly increased from 77 to 90.1% with the change of reaction pressure from 1.0 to 1.4 MPa.

Fig. 4 depicts the dependence of the formation rate of products and Cl/Cu atomic ratio from EDX analysis on time-on-stream over fresh $CuCl_2$/AC (Cu: 7 wt%) catalyst. The formation rate of DMC became higher and higher with time-on-stream, and reached an equilibrium value after 2 h reaction. It took about 3–5 h for the formation rate of MF to reach a saturation level. The level of DME was close to the results in Fig. 3B. Cl/Cu ratio decreased in the range between 0 and 2 h, and it was constant for later times on stream. DME formation rate was about 2 h to reach the saturation level, but the rate decreased slowly with the time-on-stream after that, and on the contrary, the formation rate of MF increased. These reactions seem to be strongly related to each other, since both reactions proceed via CH_3OH dehydrogenation. In this work, a 2:1 ratio of CH_3OH and CO_2 was kept during the reaction. Moreover, we carried out this reaction by performing a continuous micro-gaseous reaction. In this context, the catalytic reaction was in a dynamic balance and the total carbon balance was well kept for the reactions. Therefore, the results could be indicated by the conversion of reactants and selectivity of products.

Further analysis from Fig. 4, we could see that the catalytic stability of catalyst changed as a function of reaction time. The formation rate of DMC became higher and higher at a reaction time of 0–2 h, and then decreased gradually after 4-h reaction. The continuous decrease in catalyst activity indicated that deactivation of the catalyst proceeded gradually. Deactivation of catalyst in DMC synthesis process was likely due to a change in Cl/Cu ratio (as confirmed by the following EDX measurements). In addition, the increase in sizes of metal particles might be another factor contributing to the deactivation. These findings indicated that the deactivated catalyst could be easily regenerated by simple chemistry treatments (e.g. by HCl) and calcination, leading to the recovery of Cl/Cu ratio and re-dispersion of metal species, formation of the metal phases and recovery of the catalytic activity. The catalyst developed in this study exhibited fairly good durability as well as activity in direct synthesis of DMC under given experimental conditions.

3.2. Investigation on the surface structure and morphology of catalysts

3.2.1. EDX

The effect of the calcination temperature on the Cl/Cu ratio of the catalysts is shown in Fig. 5. The ratio decreased monotonously with increasing calcination temperature. Since the amount of copper in the catalyst was unlikely to change by calcining at a temperature below 873 K, the decrease in the ratio could be interpreted as a loss of chlorine from the catalyst. The catalyst calcined at 600 K had a Cl/Cu ratio of only 0.31, indicating species of very low Cl/Cu was present in the catalyst. The change in the Cl/Cu ratio might well interpret as a change in surface species, and the calcination temperature dominated the change. For comparison, the change of DMC formation rate is also depicted in Fig. 5. It could be seen that there was a relationship between the catalytic activity and Cl/Cu ratio. This result was coincided with Refs. [28,33].

3.2.2. TPD-NH_3

In order to investigate the relationship between the surface properties of prepared catalysts and the preparation conditions, the TPD-NH_3 test was further performed and the results are illustrated in Fig. 6. Apparently, the number of acid sites on the catalyst was strongly affected by the calcination temperature. It was found that with an increase in calcination temperature, the number of acid sites on the catalyst decreased. When the temperature reached 873 K, nearly no desorption peak could be detected, indicating that calcination temperature resulted in a decrease of surface acidity of catalyst. The weaker acid sites seem to disappear more readily upon calcination. Based on all of the experimental observations and catalytic activity investigations, it might be conclusively said that appropriate amount of surface acid sites was favorable the DMC formation.

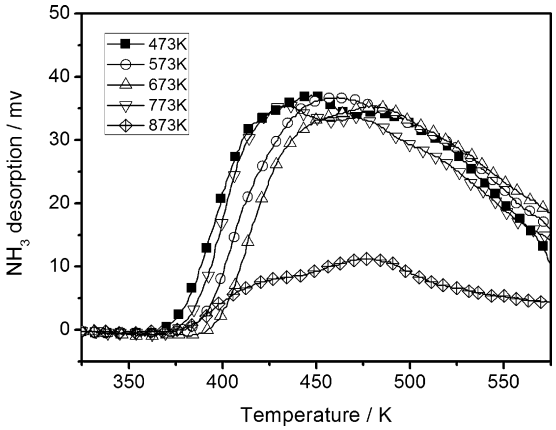

Fig. 6. TPD-NH_3 profiles of $CuCl_2$/AC catalysts (Cu: 7 wt%) with different calcination temperatures.

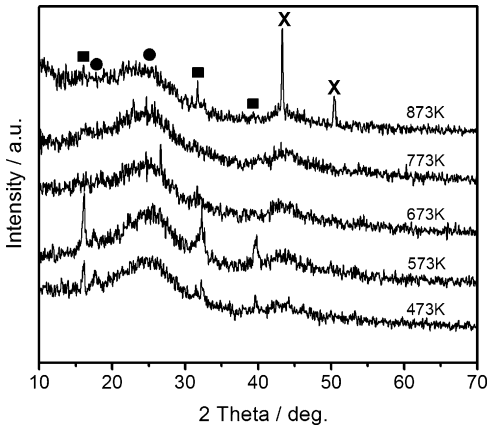

Fig. 7. XRD patterns of $CuCl_2$/AC catalysts (Cu: 7 wt%) calcined at various temperatures. (■) $Cu_2Cl(OH)_3$; (●) AC, (×) $Cu^{0/+}$.

3.2.3. XRD

The XRD patterns of $CuCl_2$/AC catalysts calcined at various temperatures are shown in Fig. 7. The broad XRD peak attributed to AC support around at $2\theta = 25^\circ$ was observed on the sample. The weak peak, at $2\theta = 18^\circ$, reflected a statistical preference for a particular inter-atomic distance of the amorphous carbon support [33]. Besides, the new peaks at $2\theta = 16.4^\circ$, $2\theta = 32^\circ$ and $2\theta = 39^\circ$ appeared. These peaks, according to JCPDS data bank (25-1427) and (30-0473), were the fingerprints of $Cu_2Cl(OH)_3$. The $Cu_2Cl(OH)_3$ came from the reaction between $CuCl_2$ and H_2O [28,33]. The intensity of these peaks became sharper as the calcination temperature increased to 573 K and no peak other than those described above was shown in the catalysts calcined at higher than 673 K. This observation illustrated the surface species on these catalysts were highly dispersed in the form of micro-crystallinity. As the calcination temperature was further increased to 773 K, additional peaks at $2\theta = 43.3^\circ$ and $2\theta = 50.48^\circ$ appeared. These peaks were identified as the peaks of metallic copper (JCPDS, 04-0836). Metallic copper was formed as a consequence of the reduction of the copper containing compounds by the carbonaceous support. The catalyst calcined at 873 K exhibited only peaks of metallic copper, showing all copper species have been reduced to metallic form at this temperature.

3.2.4. SEM

Fig. 8 shows the typical SEM images of samples calcined at 573 K (A), 673 K (B), EDX of sample B (C) and B sample suffered 3-h cat-

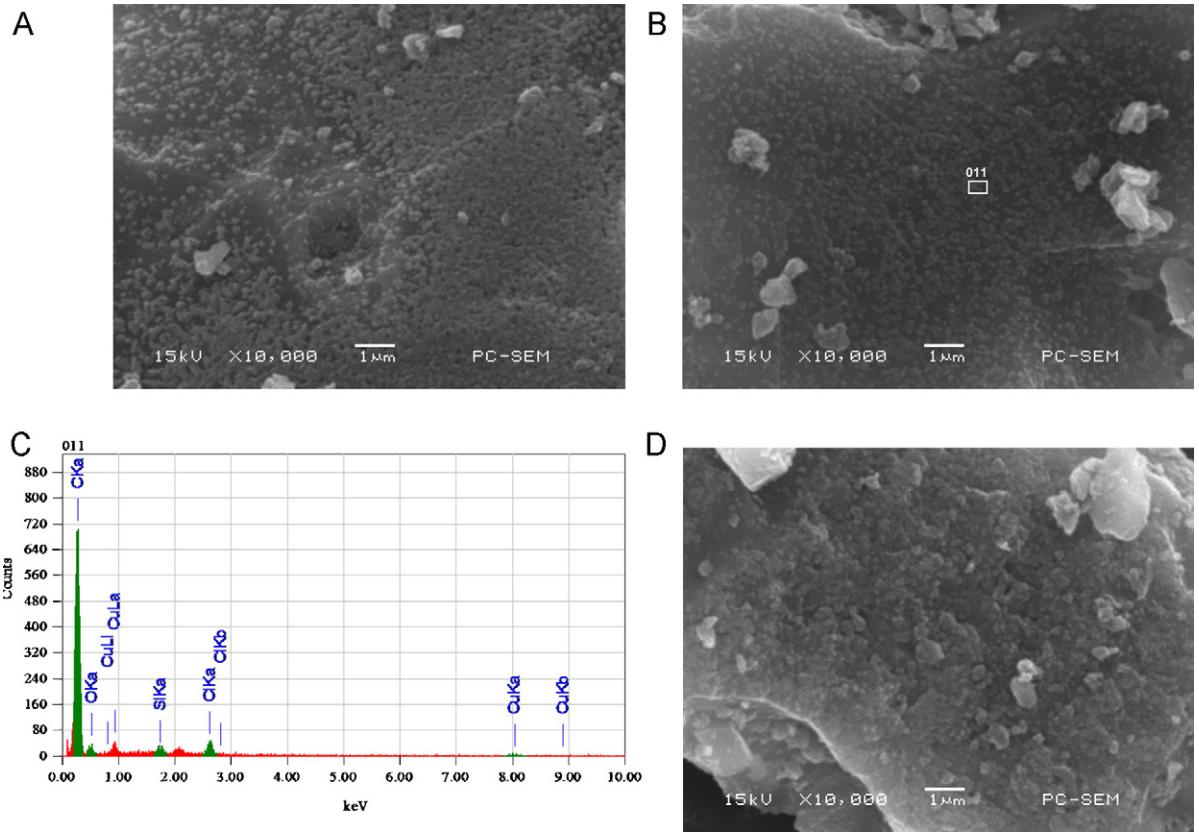

Fig. 8. SEM images of $CuCl_2$/AC (Cu: 7 wt%): (A) fresh catalyst calcined at 573 K, (B) fresh catalyst calcined at 673 K, (C) EDX pattern of catalyst B, (D) used B catalyst after 3-h reaction under the reaction conditions of $T = 393$ K; $p = 1.2$ MPa; $CH_3OH/CO_2 = 2/1$; catalyst weight 3.0 g; time-on-stream 4 h.

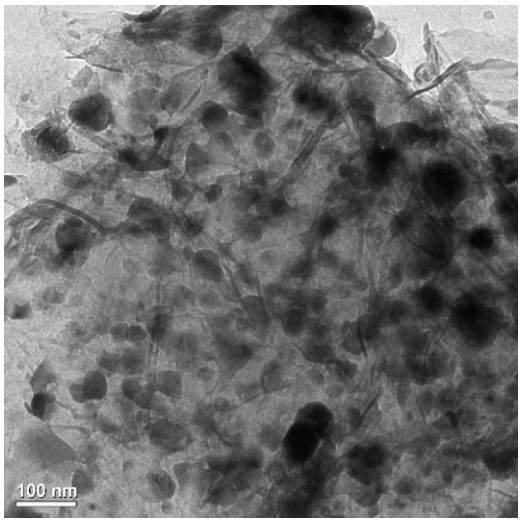

Fig. 9. TEM image of fresh $CuCl_2$/AC catalyst (Cu: 7 wt%, calcination temperature 673 K).

alytic reaction (D). In the SEM images of A and B, large particles formed in succession on the surface were observed. The dispersion was improved when calcination temperature increased from 573 to 673 K. From the fact that diffraction peaks of Cu compounds in XRD results were observed, these particles were found to be primary part on this catalyst. The energy dispersive X-ray detector (EDX) suggested that these white circular dots include C, O, Cl and Cu elements (Fig. 8C). In addition, from EDX analysis, the atomic ratio (Cl/Cu) was found to be 0.57 when an electron beam was focused on the catalyst surface. This was agreeable with the results of Fig. 5. Therefore, a major part of Cu was observed by means of either SEM or XRD. This suggested that Cu species on the catalyst before reaction was highly dispersed on the AC surface. But during the reaction, a morphological change was clearly observed. As shown in image D, active phase particles were uneven in size and exhibited some aggregation. Furthermore, a roughened structure on the AC surface was observed. This corresponded to the fact that XRD patterns of Cu–Cl–OH compounds were observed. This structural change seemed to be related to the decrease of Cl/Cu atomic ratio from 0.56 to 0.17, and furthermore, to the reaction time dependence of catalytic activity in dehydrogenation of methanol. Further observation indicated that this sample presented the broadest size distribution for active metal particles. The decrease of Cl/Cu atomic ratio and the increase in active metal particles size resulted from aggregation could be one of the reasons for catalyst deactivation.

3.2.5. TEM

The dispersion of active phase on the surface of the support is crucial to enhance the catalytic activity. As further disclosed in TEM image of the $CuCl_2$/AC catalyst (Cu: 7 wt%), the brighter grayish portions corresponded to AC support, whereas the irregular darker dots were the active metal particles (Fig. 9). It was evident that the particles were homogeneously dispersed on the surface of AC. The primary particle size estimated from the TEM image was observed in the range of 80–120 nm.

3.2.6. XPS

Fig. 10 shows the XPS spectra of two $CuCl_2$/AC catalysts, one is calcined at 673 K and the other one at 873 K. The 673 K catalyst had a large peak at 932.7 eV. Since $Cu^+2p_{3/2}$ and $Cu^0 2p_{3/2}$ had the same BE value, 932.5 eV [34]. This peak could represent either Cu^+ or Cu^0. However, the XRD analysis revealed no signal of the presence of metallic copper in this catalyst (Fig. 7). Therefore, the peak was

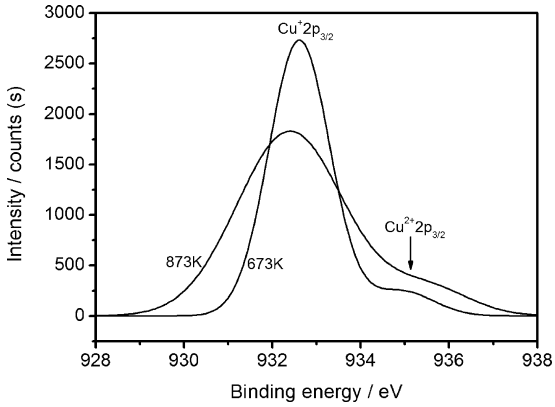

Fig. 10. XPS spectra of $CuCl_2$/AC catalysts (Cu: 7 wt%) calcined at different temperatures.

assigned solely to monovalent Cu^+, and this type of copper was the dominant copper form in the catalyst calcined at 673 K. The 873 K catalyst also had a large peak at 932.5 eV. Since the XRD analysis showed the presence of metallic copper in the catalyst (Fig. 7). Therefore, the peak represented either Cu^0 or a mixture of Cu^0 and Cu^+. In either case, the catalyst calcined at 873 K contained significantly less Cu^+ than that calcined at 673 K. Bivalent $Cu^{2+}2p_{3/2}$, with a binding energy of 935.7 eV, was shown as a shoulder in Fig. 10. By comparison, the catalyst calcined at 673 K had more Cu^{2+} than that calcined at 873 K. Since $Cu_2Cl(OH)_3$ was not observed in catalyst calcined at 873 K (Fig. 7), the Cu^{2+} in this catalyst must exist as either highly dispersed $Cu_2Cl(OH)_3$ or some other amorphous species.

4. Conclusions

In this work, one-step catalytic DMC synthesis directly from CH_3OH and CO_2 has been studied over a series of Cu-based catalysts. The effects of preparation and reaction conditions on the catalyst performance were intensively investigated in terms of DMC formation rate and DMC selectivity. The experimental results showed that the surface species of $CuCl_2$/AC catalyst was strongly affected by the loading and calcination temperature in the catalyst preparation. The optimal Cu loading and calcination temperature were found to be around 7 wt% and 673 K, respectively. The catalyst surface structure changed with time-on-stream during catalytic reaction. The activity of DMC formation rate on the $CuCl_2$/AC catalysts increased with the reaction time at the initial stage. The optimal reaction conditions for DMC synthesis reaction were found to be around 393 K and 1.2 MPa. The reaction rate was too slow below 353 K, while too much by-products was produced above 413 K. Cu^0, Cu^+ and Cu^{2+} co-existed in the form of micro-crystallinity on the catalyst and they were the active species in DMC formation. Calcining the catalyst at 673 K could maximize the presence of Cu^+ and Cu^{2+} in the catalyst, hence the activities of $CuCl_2$/AC catalyst. Moreover, maintaining proper and effective Cu structure on AC surface could promote more selective DMC formation. Combined with the merits such as the cheap nature of used materials, readily preparation and highly efficient of the as-made catalysts, we therefore expect that our results will lead to the further development of a broad new class of catalysts with enhanced properties in one-step synthesis of DMC and even trigger the preliminary nature or hot topic of new energy area.

Acknowledgements

The authors would like to thank the Key Research Fund Program of Xi-Hua University (Key Strategic Project Grant No. Z0910109) for

financial support of this research. Z. Guan thanks National University of Singapore for financial support. TPD-NH_3 and XPS tests from Si-Chuan University are gratefully acknowledged.

References

[1] Y. Ono, Appl. Catal. A 155 (1997) 133.
[2] P.G. Jessop, T. Ikariya, R. Noyori, Chem. Rev. 99 (1999) 475.
[3] D. Molzahn, M.E. Jones, G.E. Hartwell, U.S. Patent 5,387, 708 (1995).
[4] W.J. Peppel, Ind. Eng. Chem. 50 (1958) 767.
[5] J. Kizlink, Collect. Czech. Chem. Commun. 58 (1993) 1399.
[6] J. Kizlink, I. Pastucha, Collect. Czech. Chem. Commun. 60 (1995) 687.
[7] S. Fang, K. Fujimoto, Appl. Catal. A 142 (1996) L1.
[8] K. Tomishige, T. Sakaihiro, Y. Ikeda, Catal. Lett. 58 (1999) 225.
[9] C.J. Jiang, Y.H. Guo, C.G. Wang, Appl. Catal. A 256 (2003) 203.
[10] X.L. Wu, M. Xiao, Y.Z. Meng, Y.X. Lu, J. Mol. Catal. A: Chem. 238 (2005) 158.
[11] X.L. Wu, Y.Z. Meng, M. Xiao, Y.X. Lu, J. Mol. Catal. A: Chem. 249 (2006) 93.
[12] X.J. Wang, M. Xiao, S.J. Wang, Y.X. Lu, Y.Z. Meng, J. Mol. Catal. A: Chem. 278 (2007) 92.
[13] Q. Jiang, T. Li, F. Liu, Chin. J. Appl. Chem. 16 (1999) 115.
[14] K. Tomishige, K. Kunimori, Appl. Catal. A 237 (2002) 103.
[15] Z.S. Hou, B.X. Han, Z.M. Liu, Green Chem. 4 (2002) 467.
[16] C. Feng, S.H. Zhong, Catal. Today 82 (2003) 83.
[17] I.J. Drake, K.L. Fujdala, A.T. Bell, T.D. Tilley, J. Catal. 230 (2005) 14.
[18] C.F. Li, S.H. Zhong, Catal. Today 82 (2003) 83.
[19] H.J. Dai, J.H. Hafner, A.G. Rinzler, D.T. Colbert, R.E. Smalley, Nature 384 (1996) 147.
[20] D.Y. Fang, F.H. Cao, Chem. Eng. J. 78 (2000) 237.
[21] X. Ma, R. Zhao, G. Xu, F. He, H. Chen, Catal. Today 30 (1996) 201.
[22] U. Romano, R. Tesei, M.M. Mauri, P. Rebora, Ind. Eng. Prod. Dev. 19 (1980) 396.
[23] Y. Yamamoto, T. Matsuzaki, K. Ohdan, Y. Okamoto, J. Catal. 161 (1996) 577.
[24] G.L. Curuntt, U.S. Patent 4,625,044 (1986) to Dow Chemical Company.
[25] Y. Cao, J.C. Hu, P. Yang, W.L. Dai, K. Fan, Chem. Commun. (2003) 908.
[26] Z. Li, K. Xie, R.C.T. Slade, Appl. Catal. A 205 (2001) 85.
[27] P. Yang, Y. Cao, J.C. Hu, W.L. Dai, K. Fan, Appl. Catal. A 241 (2003) 363.
[28] K. Tomishige, T. Tomohiro, T. Sakaihori, S.-I. Sakai, K. Fujimoto, Appl. Catal. A 181 (1999) 95.
[29] J. Bian, M. Xiao, S.J. Wang, Y.X. Lu, Y.Z. Meng, Chem. Eng. J. 147 (2009) 287.
[30] J. Bian, M. Xiao, S.J. Wang, Y.X. Lu, Y.Z. Meng, Catal. Commun. 10 (2009) 1529.
[31] J. Bian, M. Xiao, S.J. Wang, Y.X. Lu, Y.Z. Meng, J. Colloid Interface Sci. 334 (2009) 50.
[32] J. Bian, M. Xiao, S.J. Wang, Y.X. Lu, Y.Z. Meng, Appl. Surf. Sci. 255 (2009) 7188.
[33] T.-C. Liu, C.-S. Chang, J. Chin. Inst. Chem. Eng. 38 (2007) 29.
[34] J.F. Moulder, W.F. Stickle, P.E. Sobol, K.D. Bomben, Handbook of X-ray Photoelectron Spectroscopy, Physical Electronics, Inc., Minnesota, USA, 1995, p. 220.